Lattice vibrational properties of some rare-earth antimonides: Raman scattering measurements and model theory

B. RAKSHIT[*,a], V. SRIVASTAVA, S. P. SANYAL, N. DILAWAR[b], D. VARANDANI[b], A. K. BANDYOPADHYAY[b]
Computational Physics laboratory, Department of Physics Barkatullah University Bhopal, Bhopal 462026, India
[a]*ENEA, Dipartimento Tecnologie Fisiche e Nuovi Materiali, CP 2400, 00100 Rome, Italy*
[b]*Vacuum and Pressure Standards, National Physics Laboratory, New Delhi 110012, India*

The lattice vibrational properties of three rare earth (RE) antimonides, namely LaSb, CeSb, and PrSb have been investigated experimentally, for the first time, using Raman Scattering technique at ambient pressure and room temperature. The experimental results show a single high intensity peak at zone center around 150 cm^{-1} (4.5 THz) for all the three antimonides. The experimental results have been analyzed by using breathing shell model (BSM), which includes the effect of Columb screening due to f-electron of RE ion and the breathing motion of the electron shell. The calculated phonon density of states agrees well with the measured Raman data. Calculated phonon dispersion curves for three RE antimonide compounds (LaSb, PrSb and NdSb) compare well with the available inelastic neutron scattering data. The calculated mean square displacements for these compounds show a systematic trend.

(Received December 20, 2007; accepted January 7, 2008)

Keywords: Rare earth compounds, Electron-phonon interaction, Inelastic neutron scattering

1. Introduction

Over the couple of decades, the rare-earth (RE) chalcogenides (REX, X= S, Se and Te) and pnictides (REY, Y=N, P, As and Sb) with rocksalt structure have evoked considerable interest because of their diverse electronic, optical, magnetic and phonon properties [1,2]. The peculiarities in phonon properties are generally interpreted in terms of soft phonon modes, flat optical phonon dispersion, small or negative second order elastic constants, and are believed to arise because of the presence of delocalize f-electrons of the RE ions, which during lattice vibrations, strongly interact with d-orbital of chalcogen/pnictogen ion, and thus influence both electronic and phonon structures. In view of these facts, earlier Guntherodt et al. [3] have studied the vibrational properties of Eu-Chalcogenides using Raman scattering technique. A theoretical interpretation of these results was provided by Zeyher and Kress [4] in terms of spin disorder effects by using overlap shell model. Extensive theoretical studies on the phonon properties of Eu-Chalcogenides have been reported by number of authors [5-9]. Ousaka et al. [5] have compared the Raman peaks by using breathing shell model (BSM), for EuSe. Mischenko and Kikoin [6] have reported the dispersion curves for the EuS by modifying the overlap shell model of Kress and Zeyher [4] and including the charge density deformation effects in the dynamical matrix [7]. Jha et al. [8,9] have analysed the phonon structure and Raman spectra of the Eu-Chalcogenides using three body rigid ion model (TRIM) which includes phenomenologically the effect of charge transfer due to delocalisation of f-electron of the Eu-ion.

Recently, Modukuru et al. [10] have reported the Raman scattering measurements and observed peaks at 261 cm^{-1} and 284 cm^{-1} for LaS and NdS thin films respectively. Raymond et al. [2] have investigated the anomalous phonon properties at high pressure in SmS by inelastic X-ray scattering. These authors have shown that, a significant softening of the longitudinal acoustic mode, which propagating along the (111) direction, spanning a wide q range around zone boundary. The phonon dispersion curve (PDC) for NdSb was measured long back by Wakabayashi et al. [11] using inelastic neutron scattering technique and analysed their data using screened Coulomb force model. Later McWhan et al. [12] also reported the PDC of PrSb and LaSb and showed that these antimonides have PDCs, which are nearly identical.

In the present paper, we report the lattice vibrational properties of LaSb, CeSb and PrSb, for the first time, by using Raman scattering technique. We also calculate the complete phonon dispersion curves for the above three antimonides and NdSb using breathing shell model [13], which includes phenomenologically the f-d hybridization of the electrons of the rare-earth ion. We compare the calculated PDC and density of states with the neutron and Raman scattering data. The calculated results on mean square displacements of the ions are also shown to be in good agreement with the measured results, reported earlier [11]. A brief outline of the experimental details has been given in section 2, followed by the theoretical model and the result and discussion, in sections 3 and 4, respectively.

2. Experimental technique

The polycrystalline samples of La, Ce and Pr-antimonides have been obtained from Dr. Shirotani, Japan, who has already characterized these samples by using X-ray diffraction technique [14,15] and found NaCl structure

as a stable phase at ambient pressure. A Coherent Innova 70 Argon ion laser with an excitation wavelength of 514 nm (power of 0.4 W), was used as source for Raman scattering experiment. A single stage Jobin Yvon-Spex (HR 640) monochromator is used to collect the scattered light. A thermo-electric cooled photo multiplier tube was used as detector in photon counting mode and 'Spectralink' software were used to obtain the final spectra [16]. The details of the experimental setup can be found elsewhere [17].

3. Theoretical model

The Breathing Shell Model (BSM) has been used to interpret the phonon anamolies with reasonable success [18-20] observed in several RE chalcogenides. This model takes into account the short-range electron-phonon interactions in terms of electron shell deformation. Depending upon the symmetry, the BSM includes dipolar, quadrupolar and breathing deformabilities of the electron shells of the ions. The details of physical principles of this model have been described by Singh [13]. Within the adiabatic and harmonic approximations, the dynamical matrix corresponding to BSM, can be written as:

$$D(q)=(R'+ZCZ)-(R'-ZCY)(R'+G+YCY)^{-1}(R'+YCZ) \quad (1)$$

where $R'=(R-QH^{-1}Q^{+})$; C and R are the Columb and short-range repulsive interaction matrices respectively. Q is (6×2) matrix representing the interactions between the ion displacements and breathing mode variables. The H is a (2×2) matrix and represents the interactions between the breathing mode variables of different ions in the lattice. These matrices are written as [13]

$$Q=\begin{bmatrix} 0 & D \\ D & 0 \end{bmatrix} \quad (2)$$

where D is three vector breathing matrix

$$D= - iA\begin{bmatrix} \sin q_\alpha r_o \\ \sin q_\beta r_o \\ \sin q_\gamma r_o \end{bmatrix} \quad (3)$$

and

$$H=\begin{vmatrix} H(11) & H(12) \\ H(21) & H(22) \end{vmatrix} \quad (4)$$

with

$$H(11)==3A+G_1, H(22)=3A+G_2,$$

$$H(12)=H(21)=A\left(\cos q_\alpha r_o + \cos q_\beta r_o + \cos q_\gamma r_o\right) \quad (5)$$

G and A are the diagonal matrices and represent the core-shell interaction and shell charge, respectively. The G_1 and G_2 can be expressed as

$$\frac{\partial^2 V_{CS}^{(1)}}{\partial r^2}=\frac{e^2}{V}G_1 \quad (6)$$

$$\frac{\partial^2 V_{CS}^{(2)}}{\partial r^2}=\frac{e^2}{V}G_2 \quad (7)$$

where $V_{CS}^{(1)}$ and $V_{CS}^{(2)}$ are the core-shell interaction potentials for ion number 1 and 2 respectively. The parameters involved in the dynamical matrix $\boldsymbol{D}(\boldsymbol{q})$ are determined by their relation with some macroscopic experimental data, i.e. elastic constant, dielectric constant and zone center phonon frequencies. In order to minimize the number of parameters, we have assumed the shell charges, $Y_1=Y_2=Y$. The input data and the output model parameters are tabulated in Table 1 and 2.

The validity of any model can be tested by predicting the eigen vectors and possibly through the Debye-Waller factor or mean square displacement (MSD) of ions, which are directly expressible in terms of eigen vectors. Cochran [21] and Leigh et al. [22] emphasized the necessity of the eigenvectors as they provide more stringent test of any model. The mean square displacements of *k*-th particle is expressed in terms of the phonon frequencies and eigenvectors as

$$\left\langle u^2 \right\rangle_k = \frac{\hbar}{Nm_k}\sum_q \sum_j \frac{\left|e(k/q,j)\right|^2}{\omega_j(q)}\left[n(\omega_j(q))+\frac{1}{2}\right] \quad (8)$$

Here, $\omega_j(q)$ is the eigen frequency of *j*-th branch for wave vector $\boldsymbol{q}$ with corresponding eigenvectors $e(k/q,j)$ of the dynamical matrix D($\boldsymbol{q}$). The quantity $n(\omega_j(q))$ is the phonon occupation number,

$$n(\omega_j(q))=\left[\exp(\hbar\omega_j(q)/k_BT)-1\right]^{-1} \quad (9)$$

with k_B Boltzmann constant, and T is the absolute temperature.

4. Results and discussion

In the present paper, we report the vibrational properties for the three RE-Sb compounds using Raman scattering technique at ambient pressure and temperature and analysed these data using the breathing shell model (BSM). The Raman spectra for LaSb, CeSb and PrSb are presented in Fig. 1(a) to 1(c), which show a sharp peak at 4.56, 4.33 and 4.36 THz, respectively along with few other small peaks. In Fig. 1 (a), (b) and (c), there are peaks in the higher energy regions at 8.21, 7.62 and 7.45 THz, respectively. These peaks may arise due to oxygen impurity in all the RE-Sb compounds. Since these compounds are semi-metallic in nature, one expects the ω_{LO} and ω_{TO} to be degenerate, as shown by neutron scattering results [11, 12]. We assign these peaks to originate from ω_{LO} (or ω_{TO}). A critical assessment of the Raman peaks reveals that the half width of the peak for

LaSb is quite large in magnitude, as compared to Ce and Pr. However, the width is nearly identical for Ce and Pr antimonides because of their nearly identical masses. The optical response of the RE antimonides to the laser wavelength (and power) used in the present experiment, might be responsible for the peak broadening.

In order to understand the Raman spectra and earlier neutron scattering results [11, 12] we first calculated the phonon dispersion curves for four RE-Sb systems, namely LaSb, CeSb, PrSb and NdSb, by using breathing shell model (BSM) which has been used earlier by Jha and coworker [18-20] to explain satisfactorily the anomalous phonon properties in rare earth chalcogenides and pnictides. The input constants and derived model parameters are listed in Tables 1 and 2, respectively. We have considered the second neighbor short range interactions for the RE ions as they have significant effect on the dynamical matrix due to the presence of delocalized f-electrons. The same for Sb ions is neglected. In Fig. 2(a) to 2(d) we present the calculated phonon dispersion curves for the above four compounds and compare them with the present Raman spectroscopic and available inelastic neutron scattering results, reported earlier by Wakabayashi and Furrer [11] and McWhan et al [12] in the principle symmetry directions. Fig. 2(a) reveals that the theoretical phonon dispersion curves for LaSb are in good agreement with the experimental data along (q 0 0) and (q q 0) directions for LA and TA modes. However, our calculated results for optical modes along the Brillouin zone deviate from the measured ones. On the other hand the agreement between the calculated and measured phonon modes (both acoustic and optical) in the case of NdSb is fairly good, as is revealed from Fig. 2(d). In our calculations, we have, however failed to notice the crossover of TO and LA at (.5 .5 .5), which is reported in neutron scattering experiment. The effect of electronic polarizabilities of both RE and Sb ions are quite obvious and can be marked around the X-point of the Brillouin zone, where LA branch shows a hump around (.8 0 0) and comes down sharply at X-point. As in other RE-compounds [2], the LA and TA branches are nearly degenerate along (q q q) direction. Strong electron-phonon interactions might be responsible for such peculiar behaviors.

Table 1. Input constants for calculation of model parameters.

Parameters	LaSb	CeSb	PrSb	NdSb
a (Å)	6.49 [c]	6.42 [c]	6.384 [d]	6.328 [a]
C_{11}(dyn/cm^2)	1.4 [b]	1.4	1.4 [b]	1.7 [a]
C_{12} (dyn/cm^2)	0.2 [b]	0.20	0.20 [b]	0.22 [a]
C_{44} (dyn/cm^2)	0.21 [b]	0.21	0.21 [b]	0.25 [a]
$\nu_{LO}(\Gamma)$ (THz)	4.510 [*]	4.346 [*]	4.369 [*]	4.087 [a]
α_1 (Å)^3	0.64	0.62	0.58	0.54
Z_m [**]	0.326	0.394	0.409	0.369
$\varepsilon_o = \varepsilon_\infty$	1.510	1.502	1.494	1.452

[*] Present experimental Raman data.
[**] Present calculations.
[a]Ref. [11]; [b]Ref. [12]; [c]Ref. [23]; [d]Ref. [24].

Table 2. Model Parameters for BSM (all Parameters are in the units of e^2/V, Y is in units of e and α_2 is in units of (Å)^3. A_{12} and B_{12} are the short range force constant between the first neighbours, for dissimilar atoms. A_{11} and B_{11} for the similar atoms.

Parameters	LaSb	CeSb	PrSb	NdSb
A_{12}	34.908	36.133	38.476	40.464
B_{12}	4.558	6.38	7.09	3.818
A_{11}	21.396	20.723	21.323	25.968
B_{11}	-7.6754	-8.906	-9.525	-6.590
α_2	2.039	2.088	2.051	1.922
Y	-1.5354	-1.302	-1.323	-1.133
G_1	251.71	180.88	196.138	150.571
G_2	78.98	53.71	55.44	43.362

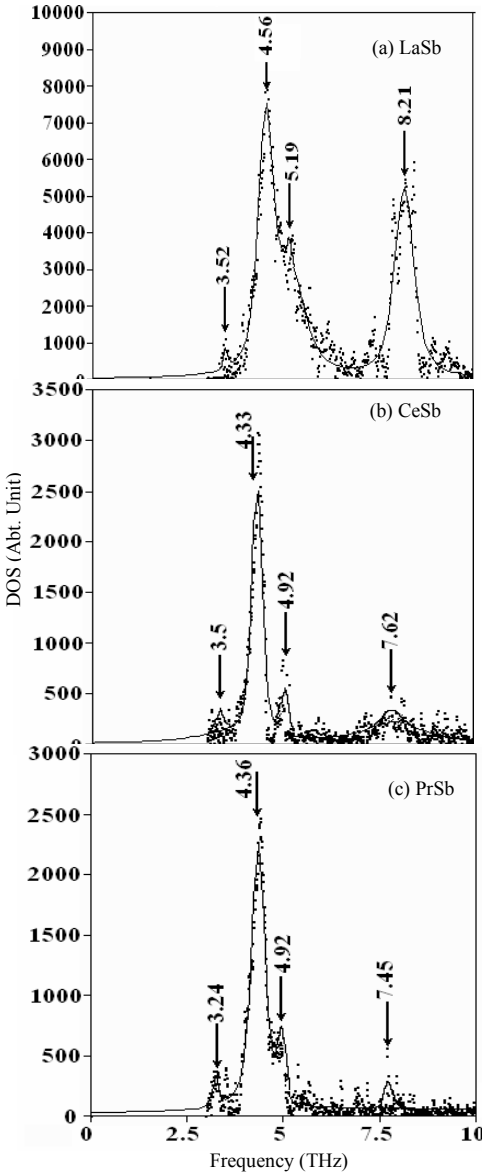

Fig. 1. Raman spectrum of (a) LaSb, (b) CeSb, and (c) PrSb. The prominent peaks around 4.4 THz is due to $\omega_{LO} = \omega_{TO}$.

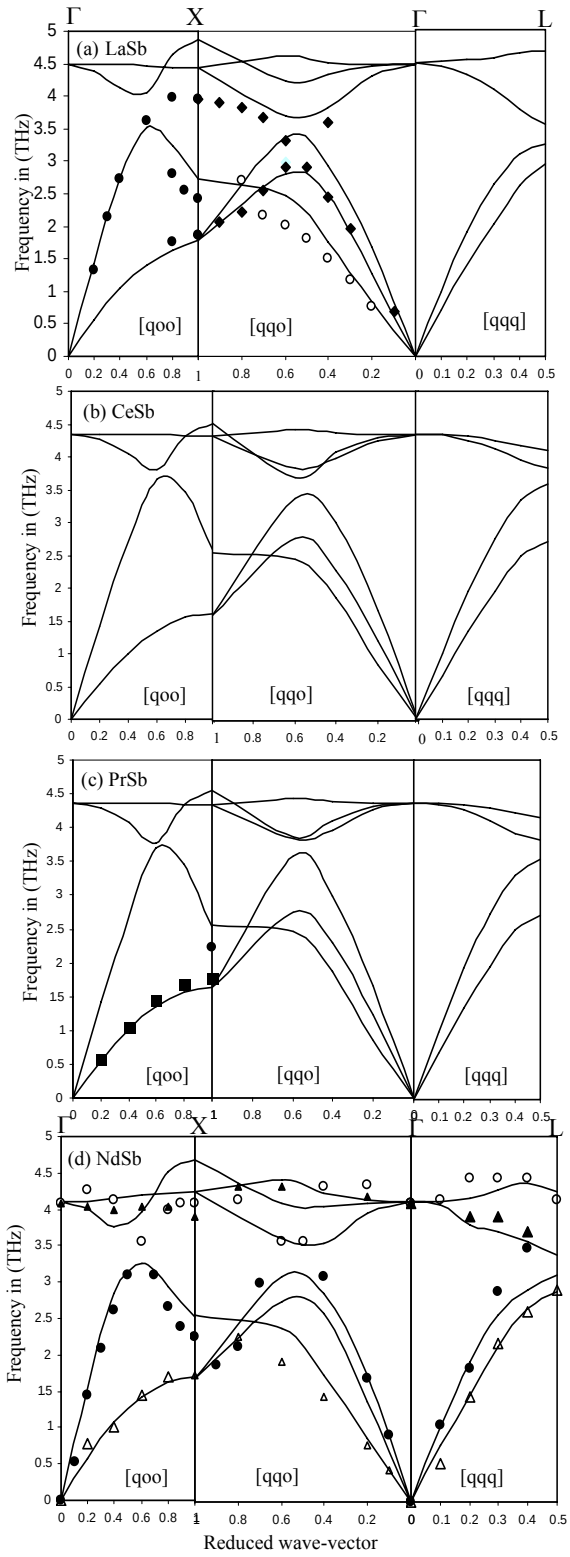

Fig. 2. Phonon Dispersion Curve for (a) LaSb, (b) CeSb, (c) PrSb and (d) NdSb. The open and closed symbols are the experimental data of NdSb, PrSb and LaSb taken from Ref [11, 12], respectively. The solid lines are theoretical (BSM) results.

In order to compare our results with the measured Raman spectra in Figs. 3(a) to 3(d) we have plotted the phonon Density of States (DOS) for the four RE-antimonides compounds. It is seen from Figs. 3(a) to 3(c) that the calculated DOS reproduce the peak positions excellently for La, Ce and Pr-antimonide compounds. The major Raman peaks for LaSb, CeSb and PrSb are centered at 4.56, 4.33 and 4.36 THz. The corresponding calculated values in DOS are 4.49, 4.27 and 4.24 THz agree excellently with the experimental ones. The observed smaller peaks in Raman spectra for LaSb, CeSb and PrSb at 3.52, 3.50 and 3.24 THz, respectively match with the calculated DOS value centered at 3.79, 3.25 and 3.21 THz. For NdSb we obtain a sharp DOS peak at 4.07 THz for ω_{TO} and other peaks are at lower frequency range at 3.75, 3.4, 2.7 and 2.2 THz.

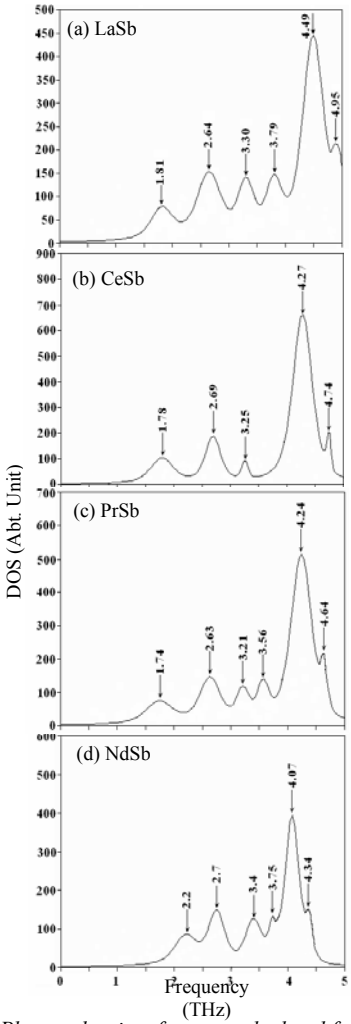

Fig. 3. Phonon density of states, calculated from BSM, for antimonides of La, Ce, Pr and Nd.

These sharp peaks are due to electron-phonon interaction, resulting from ω_{TO} modes at the zone center. In addition, we have also obtained few more peaks in DOS plot in the lower energy side. In addition, for the sake of completeness, we have calculated the mean square displacement (MSD) of various ions for all the four RE-

antimonides using Eq. (8) at different temperatures, for which the eigenvalues and eigenvectors are obtained by solving the equation, $\left|D(q)-\omega^2 MI\right|=0$, for 48 non-equivalent wave vectors in the first Brillouin zone. In Fig. 4 we have plotted MSD as function of temperature for all the four compounds. The magnitude of MSD is larger for antimonide ions as compared to the RE ion, because of mass. The theoretical values fitted to neutron scattering results for NdSb, are also compared with our theoretical results in Fig. 4(d) [11]. We have achieved a good agreement with our calculations.

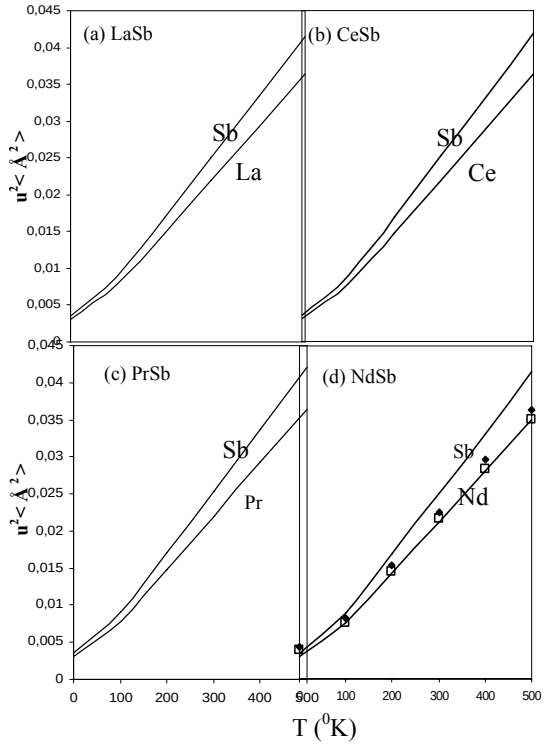

Fig. 4. Temperature dependence of mean square displacement <u²> for the RE-Sb compounds for (a) LaSb, (b) CeSb, (c) PrSb and (d) NdSb. In 4(d) the symbols show the experimental values and are taken from Ref [11]; ▲Sb ion, □ Nd ion.

5. Conclusions

We have measured the zone center optical modes of three RE-Sb compounds through Raman scattering technique. A theoretical model is being used to interpret the results of our own measurements and those already reported from neutron scattering experiments. We have observed that the RE-Sb compounds, investigated in this work, are semi-metallic in nature and the optical modes at zone center are energetically degenerate, similar to those already reported in literature.

Acknowledgements

The authors are extremely grateful to Dr. A K Arora and Dr. T. R. Ravindran (IGCAR, Kalpakkam) and to Dr. P. K. Jha for useful discussions. VS is thankful to DST for the Young Scientist award under fast track scheme (Ref. No. SR/FTP/PS-30/2005).

References

[1] C. M. Verma, Rev. Mod. Phys. **48**, 219 (1976); J. M. Robinson, Rep. In. Phys. **51**, 1 (1979); P. Wachter, K. A. G. Schineider Jr. and L. Eying (Eds.), Hand Book on Phys. and Chem. of Rare Earths, North Holland, Amsterdam, 1994, vol. 19.
[2] P. K. Jha, S. P. Sanyal, R. K. Singh. Proc. INSA **68 A**, 57 (2002); and references therein; S. Raymond, J. P. Rueff, M. D. Astuto, D. Braithwaite, M. Krisch, J. Flouquet Phys. Rev. **B 66**, 220301 (R) (2002).
[3] G. Guntherodt, A. Jayaraman, W. Kress, H. Bilz, Phys. Lett. **20**, 824 (1981).
[4] R. Zeyher, W. Kress, Phys. Rev. **B 20**, 2850 (1979).
[5] Y. Ousaka, O. Sakai, M. Tachiki, Solid State Commun. **23**, 589 (1977).
[6] A. S. Mischenko, K. A. Kikoin, J. Phys. (Condensed Matter) **3**, 5937 (1991).
[7] A. S. Mischenko, K. A. Kikoin, Sov. Phys. JETP **67**, 2309 (1988).
[8] P. K. Jha, S. P. Sanyal, Ind. J. Pure and Appl. Phys. **32**, 824 (1994).
[9] U. K. Sakalle, P. K. Jha, S. P. Sanyal, Bull. Mat. Sc. **23**, 233 (2000); U. Sakalle, Ph. D. Thesis, Barkatullah University Bhopal (1999).
[10] Y. Modukuru, J. Thachery, H. Tang, A. Malhotra, M. Cahay, P. Boolchand, J. Vac. Sci. Technol. B **19(5)**, 1958 (2001).
[11] N. Wakabayashi, A. Furrer, Phys. Rev. **B 13**, 4343 (1976).
[12] D. B. McWhan, C. Vettier, L. D. Longinotti, G. Shirane, Phys. Rev. **B 18**, 4540 (1978).
[13] R. K. Singh, Phys. Rep. **85**, 259 (1982).
[14] I. Shirotani, J. Hayashi, K. Yamanashi, N. Ishimatsu, O. Shimomura, T. Kikegawa, Phys. Rev. **B 64**, 132101 (2001).
[15] I. Shirotani, K. Yamanashi, J. Hayashi, Y. Tanaka, N. Ishimatsu, O. Shimomura, T. Kikegawa, J. Phy. Condensed Matter **13**, 1939 (2001).
[16] Vipul Srivastava, Ph. D. Thesis, Barkatullah University, Bhopal, (2005).
[17] A. K. Bandyopadhyay, N. Dilawar, A. Vijaykumar, D. Varandani, D. Singh, Bull. Mater. Sci. **21**, 433 (1998).
[18] P. K. Jha, S. P. Sanyal, Phys. Rev. B **46**, 3664 (1992).
[19] P. K. Jha, S. P. Sanyal, Physica B **216**, 125 (1995).
[20] M. Aynyas, P. K. Jha, S. P. Sanyal, Ind. J. Pure and Appl. Phys. **43**, 109 (2005).
[21] W. Cochran, Acta Cryst. A **27**, 556 (1971).
[22] R. S. Leigh, B. Szigeti, V. K. Tiwary, Proc. Roy. Soc. A **320**, 505 (1970).
[23] J. M. Leger, D. Ravot, J. Rossat Mignod, J. Phys. C **17**, 4935 (1984).
[24] J. Hayashi, I. Shirotani, Y. Tanaka, T. Adachi, O. Shimomura, T. Kikegawa, Solid State Commun. **114**, 561 (2000).

*Corresponding author: bipulrr@yahoo.co.in